Korean Journal of Geomatics
Vol. 4, No. 1 / November 2004
pp. 31~37

The Evaluations of Sensor Models for Push-broom Satellite Sensor

Suk-Kun LEE* and Hoon CHANG**

Abstract

The aim of this research is comparing the existing approximation models (e.g. Affine Transformation and Direct Linear Transformation) with Rational Function Model as a substitute of rigorous sensor model of linear array scanner, especially push-broom sensor. To do so, this research investigates the mathematical model of each approximation method. This is followed by the assessments of accuracy of transformation from object space to image space by using simulated data generated by collinearity equations which incorporate or depict the physical aspects of linear array sensor.

Keywords : *Affine Transformation, Direct Linear Transformation, Rational Function, Collinearity Equation*

1. Introduction

Like SPOT and IKONOS current launched satellites have preferably equipped of linear CCD arrays in imaging system designed to acquire digital format of imagery. Push-broom (e.g. SPOT and IKONOS), three-line (e.g. MOM), and panoramic linear array are three types of imaging systems equipped linear CCD array, which are classified by angles between flight direction and linear array in image plane. Unlike frame camera system, linear array scanner brought the complexity in physical modelling of the sensor. It is inherently comes from the dynamic conditions (e.g. sensor movements during exposure time) resulted in distortions that can not find in frame imagery. In this research, we selected push-broom scanners as a target sensor to be studied since it can reflect the general aspects of linear scanner sensor.

For the certain application that desired only low or medium level accuracy, the complexity and rigorousness of physical modelling of push-broom sensor may leads people rather to use a coarse approximate method (e.g. 2D affine transformation) (Okamoto et al, 1999) for representation of relationship between image space and object space. Another alternatives for improving the accuracy can be found in the Rational Function Model (RFM) such as Direct Linear Transformation (DLT) (El-Manadili and Novak, 1996) and higher order RFM. These types of generic models is not required knowledge of the orbital information and Exterior Orientation Parameters (EOP) for restitute the relationship between image space and object space.

Since OpenGISTM Consortium (OGC) proposed the RFM as one of the Earth image geometry model (OGC, 1999), researchers including Tao et al. (2000a), Dowman et al. (2000), and Yang (2000) reported the feasibility of using RFM for resection and space intersection problems which are the common and basic tasks in photogrammetry. Di et al. (2000) applied RFM for deriving shorelines from simulated IKONOS satellite images. This research explicitly describes the form of upward (object to image space transformation) and downward (image to object space transformation) RFM. The majority of these researches are mostly come up with the reasonable accuracy of resection or space intersection by using tens of control points. However, we may encounter the case of only few control points available. In this case, we may not solve the polynomial coefficients of RFM (e.g. 78 parameters for 3rd order ratios of polynomials).

This research focuses on comparing aforementioned methods (affine, DLT, and RFM) in terms of level of

*Member, Plural Prof., Yeungnam College of Science and Technology (E-mail : aimsk@hitel.net)
**Senior Lecturer, SungKyunKwan University (E-mail : hchang@skku.edu)

The manuscript for this paper was submitted for review on October 1, 2004 / accepted on October 17, 2004

accuracy and parameters involved by using simulated data for push-broom sensor model. The rest of this paper will present Chapter 2 which explores the details of mathematical model of each method to utilize the relationship between image space and object space. This is followed by Chapter 3 presenting the experiments and results. Chapter 4 summarizes the analysis of this study and suggests the future study.

2. Mathematical Model

2.1 Rigorous and Robust Model

The perspective relationship between image and object space can be established through collinearity equations as follows:

$$x_a = x_p - c\frac{r_{11}(X-X_0)+r_{21}(Y-Y_0)+r_{31}(Z-Z_0)}{r_{13}(X-X_0)+r_{23}(Y-Y_0)+r_{33}(Z-Z_0)} \quad (1)$$

$$y_a = y_p - c\frac{r_{12}(X-X_0)+r_{22}(Y-Y_0)+r_{32}(Z-Z_0)}{r_{13}(X-X_0)+r_{23}(Y-Y_0)+r_{33}(Z-Z_0)} \quad (2)$$

where, (x_a y_a) are the metric image coordinates of point a, (c) is the principal distance, (x_p y_p) are the metric image coordinates of principal points, (X, Y, Z) are the ground coordinates of point A corresponding image point a, (X_0, Y_0, Z_0) are the ground coordinates of perspective center during exposure time, (r11, ..., r33) are the elements of rotation matrix.

However, equation (1) and (2) describe the relationship between frame image and object space through the use of points. For the push-broom imagery, the perspective center is moving during the exposure time as illustrated in figure (1). This introduces the necessity of incorporation of time variable into the relationship between image coordinate system and object coordinate system. Figure (2) shows the relationship image and object space for the push-broom scanner (Lee, 2002).

Consequently, aforementioned collinearity equations need to be modicmlqtd for applying them to push-broom imagery as follows:

$$x_a = x_p - c\frac{r^t_{11}(X-X^t_0)+r^t_{21}(Y-Y^t_0)+r^t_{31}(Z-Z^t_0)}{r^t_{13}(X-X^t_0)+r^t_{23}(Y-Y^t_0)+r^t_{33}(Z-Z^t_0)} \quad (3)$$

$$y_a = y_p - c\frac{r^t_{12}(X-X^t_0)+r^t_{22}(Y-Y^t_0)+r^t_{32}(Z-Z^t_0)}{r^t_{13}(X-X^t_0)+r^t_{23}(Y-Y^t_0)+r^t_{33}(Z-Z^t_0)} \quad (4)$$

Where, (x_a, y_a) are the photo coordinates of point a and ya = 0, (c) is the principal distance, (x_p, y_p) are the photo coordinates of principal points, (X, Y, Z) are the ground coordinates of point A corresponding image point a, (X^t_0, Y^t_0, Z^t_0) are the ground coordinates of perspective center at time t, (r^t_{11}, ..., r^t_{33}) are the elements of rotation matrix at time t.

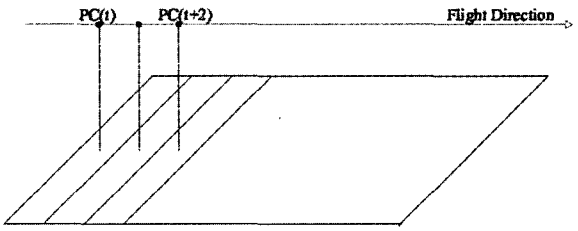

Fig. 1. Push-broom imaging system.

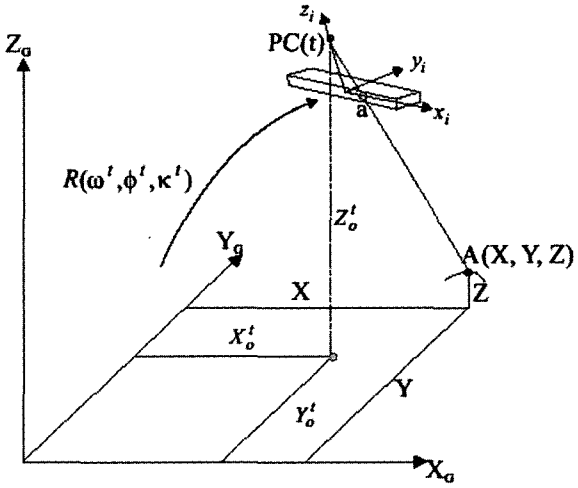

Fig. 2. The relationship between image space and object space in push-broom scanner.

2.2 Rational Function Model

2.2.1 Ratios of polynomials

This generic sensor model uses a ratio of two polynomial functions to compute the row and column locations in image of object points. All four polynomials are function of ground coordinates of points. Usually, each polynomial has 20 coefficient of polynomial. In the equations describing the relationship between image coordinates and ground coordinates of points, the coordinates have normalized coordinates which have range of -1 to 1 over an image segment. For each image segment, the ratios of polynomials are defined as follow equation (5) and (6):

$$r_n = \frac{p_1(X_n, Y_n, Z_n)}{q_1(X_n, Y_n, Z_n)} \quad (5)$$

$$c_n = \frac{p_2(X_n, Y_n, Z_n)}{q_2(X_n, Y_n, Z_n)} \quad (6)$$

Where, (r_n, c_n) are normalized pixel coordinates (row, column), (X_n, Y_n, Z_n) are the normalized ground coordinates (easting, northing, height).

The polynomials described in equation (5) and (6) have the form:

$$p_1 = \sum_{i=0}^{m1}\sum_{j=0}^{m2}\sum_{k=0}^{m3} a_{ijk} X_n^i Y_n^j Z_n^k \quad (7)$$

$$p_2 = \sum_{i=0}^{m1}\sum_{j=0}^{m2}\sum_{k=0}^{m3} c_{ijk} X_n^i Y_n^j Z_n^k \quad (8)$$

$$q_1 = \sum_{i=0}^{m1}\sum_{j=0}^{m2}\sum_{k=0}^{m3} b_{ijk} X_n^i Y_n^j Z_n^k \quad (9)$$

$$q_2 = \sum_{i=0}^{m1}\sum_{j=0}^{m2}\sum_{k=0}^{m3} d_{ijk} X_n^i Y_n^j Z_n^k \quad (10)$$

Where, a_{ijk}, b_{ijk}, c_{ijk}, and d_{ijk} are the polynomial coefficients.

For uses of polynomials, the maximum powers of each ground coordinate (m1, m2, m3, n1, n2, and n3) are limited to 3. Also, the total power of all three ground coordinates is limited to 3. In other words, the polynomial coefficients are to be zero whenever i + j + k > 3. With aforementioned limitation of powers, we can rewrite equations (5) and (6) as follows:

$$r_n = \frac{p_1(X_n, Y_n, Z_n)}{q_1(X_n, Y_n, Z_n)} = \frac{(1, X, Y, Z, \cdots, X^3, Y^3, Z^3)\cdot(a_0, a_1, \cdots, a_{19})^T}{(1, X, Y, Z, \cdots, X^3, Y^3, Z^3)\cdot(1, b_1, \cdots, b_{19})^T} \quad (11)$$

$$c_n = \frac{p_2(X_n, Y_n, Z_n)}{q_2(X_n, Y_n, Z_n)} = \frac{(1, X, Y, Z, \cdots, X^3, Y^3, Z^3)\cdot(c_0, c_1, \cdots, c_{19})^T}{(1, X, Y, Z, \cdots, X^3, Y^3, Z^3)\cdot(1, d_1, \cdots, d_{19})^T} \quad (12)$$

2.2.2 Normalization of coordinates

In this section, the normalization steps are presented. For each image segment, the ground coordinates are offset and scaled to fit the range of -1 to 1. The normalize ground coordinates are computed as follows (OGC, 1999):

$$X_n = \frac{X_u - X_o}{X_s}$$

$$Y_n = \frac{Y_u - Y_o}{Y_s}$$

$$Z_n = \frac{Z_u - Z_o}{Z_s} \quad (13)$$

Where, (X_n, Y_n, Z_n) are the normalized ground coordinates, (Xu, Yu, Zu) are the un-normalized ground coordinates, (Xo, Yo, Zo) are the offset values for ground coordinate system, (Xs, Ys, Zs) are the scale values for ground coordinate system.

In the same fashion, the image coordinates can be normalized as follows:

$$r_n = \frac{r_u - r_o}{r_s}$$

$$c_n = \frac{c_u - c_o}{c_s} \quad (14)$$

Where,

(r_n, c_n) are the normalized image coordinates, (r_u, c_u) are the un-normalized image coordinates, (r_o, c_o) are the offset values for image coordinate system, (r_s, c_s) are the scale values for image coordinate system.

The general aspects of RFM can be explained as follows:

- It is a generic sensor model which does not require the trajectory information and physical sensor information.
- The uses of this model can be limited by using of image sections splitted from original scene of image.
- If we have to estimate the polynomial parameters (e.g. Unlike IKONOS, SPOT scene does not come along with polynomial coefficients), RFM model becomes less practical model for the area which does not have enough control points.

2.3 Affine Transformation

Some studies have presented that acceptable accuracy of results for rectification using 2D affine model can be achieved. The general form of 2D affine model, which is also referred as Linear polynomials (OGC, 1999), for 3D analysis of linear scanner imagery can be expressed as follows (Okamoto and others, 1999):

$$x_i = a_0 + a_1 X_i + a_2 Y_i + a_3 Z_i$$
$$y_i = b_0 + b_1 X_i + b_2 Y_i + b_3 Z_i \quad (15)$$

Where, x_i and y_i are the image coordinates of point i, X_i, Y_i, and Z_i are the object coordinates of point i, and (a_0, ..., b_3) are the affine parameters to be estimated.

The capabilities of this model can be found in following facts:

- It has the simple form of equations and is easy to implement to obtain the results.
- It could be applicable for relatively flat surface which does not have the undulation of terrains.
- It is a simplest form of generic sensor model which has zero order of polynomials in denominators and 1st order of polynomials in numerators in equation (11) and (12).
- The accuracy of this model generally less accurate than the collinearity based rigorous model.

2.4 Direct Linear Transformation

DLT relates the measured stage coordinates on the comparator directly to the ground coordinates. DLT can be derived by comparing the affine transformation and the collinearity equations together, which yields equation (16):

$$x_a = x_p - c_x \frac{r_{11}(X-X_0)+r_{21}(Y-Y_0)+r_{31}(Z-Z_0)}{r_{13}(X-X_0)+r_{23}(Y-Y_0)+r_{33}(Z-Z_0)}$$
$$y_a = y_p - c_y \frac{r^t_{12}(X-X^t_0)+r^t_{22}(Y-Y^t_0)+r^t_{32}(Z-Z^t_0)}{r^t_{13}(X-X^t_0)+r^t_{23}(Y-Y^t_0)+r^t_{33}(Z-Z^t_0)} \quad (16)$$

Where, (x_a, y_a) are the metric image coordinates of point a, (c_x, c_y) are the principal distance with respect to x and y direction, respectively, (x_p, y_p) are the metric image coordinates of principal points, (X, Y, Z) are the ground coordinates of point A corresponding image point a, (X_o, Y_o, Z_o) are the ground coordinates of perspective center during exposure time, (r_{11}, ..., r_{33}) are the elements of rotation matrix.

As one can note that there are two principal distances (cx cy), which is different from regular collinearity equation. These two principal distances compensate for the two scale factors of the affine transformation. The shift of the affine transformation is compensated by the coordinates of the principal points (x_p, y_p). In addition, the rotation are compensated for by the κ rotation which is the angle with respect to Z-axis of ground coordinate system. Equation (16) can be rewritten as follows:

$$x_a = \frac{L_1X+L_2Y+L_3Z+L_4}{L_9X+L_{10}Y+L_{11}Z+1}$$
$$y_a = \frac{L_5X+L_6Y+L_7Z+L_8}{L_9X+L_{10}Y+L_{11}Z+1} \quad (17)$$

Where, $L_1 = (xp \cdot r_{13}-c_x \cdot r_{11})/L$, $L_2 = (x_p \cdot r_{23}-c_x \cdot r_{21})/L$, $L_3 = (x_p \cdot r_{33}-c_x \cdot r_{31})/L$, $L_4 = x_p+c_x(r_{11}Xo+r_{21}Yo+r_{31}Zo)/L$, $L_5 = (y_pr_{13}-c_yr_{12})/L$, $L_6 = (y_pr_{23}-c_yr_{22})/L$, $L_7 = (y_pr_{33}-c_yr_{32})/L$, $L_8 = y_p+c_y(r_{12}Xo+r_{22}Yo+r_{32}Zo)/L$, $L_9 = r_{13}/L$, $L_{10} = r_{23}/L$, $L_{11} = r_{33}/L$, and $L = -(r_{13}Xo+r_{23}Yo+r_{33}Zo)$.

Equation (17) is linear in the unknown parameters. This can be done by rewriting equation (17) as follows:

$$x_a = XL_1 + YL_2 + ZL_3 + L_4 - x_aXL_9 - x_aYL_{10} - x_aZL_{11} + e_{x_a}$$
$$y_a = XL_5 + YL_6 + ZL_7 + L_8 - y_aXL_9 - y_aYL_{10} - y_aZL_{11} + e_{y_a} \quad (18)$$

Where, (e_{xa} e_{ya}) are the error vectors of observations of x_a and y_a, respectively.

To solve the unknown coefficients, we need to at least 6 points. Thus, we end up with 12 equations for 11 parameters to be solved. Those equations can be solved for by least square adjustment. Once the 11 parameters have been estimated, the EOP as well as IOP can be computed as follows:

$$L = -\frac{1}{\sqrt{L_9^2+L_{10}^2+L_{11}^2}} \quad (19)$$
$$x_p = (L_1 \cdot L_9 + L_2 \cdot L_{10} + L_3 \cdot L_{11}) \cdot L^2 \quad (20)$$
$$y_p = (L_5 \cdot L_9 + L_6 \cdot L_{10} + L_7 \cdot L_{11}) \cdot L^2 \quad (21)$$
$$c_x = \sqrt{(L_1^2+L_2^2+L_3^2)-x_p^2} \quad (22)$$
$$c_y = \sqrt{(L_5^2+L_6^2+L_7^2)-x_p^2} \quad (23)$$
$$\phi = \sin^{-1}(L_9 \cdot L) \quad (24)$$
$$\omega = \tan^{-1}(-\frac{L_{10}}{L_{11}}) \quad (25)$$
$$\varkappa = \cos^{-1}(\frac{r_{11}}{\cos\phi}) \quad (26)$$
$$r_{11} = L\frac{(x_p \cdot L_9 - L_1)}{c_x} \quad (27)$$
$$\begin{bmatrix} X_o \\ Y_o \\ Z_o \end{bmatrix} = -\begin{bmatrix} L_1 & L_2 & L_3 \\ L_5 & L_6 & L_7 \\ L_9 & L_{10} & L_{11} \end{bmatrix} -1 \begin{bmatrix} L_4 \\ L_8 \\ 1 \end{bmatrix} \quad (28)$$

If we explore equation (17), 10 parameters(xp, ,..., Zo) in equation (16) replaced by 11 parameters (L1, ... L11). The additional parameter can be viewed as compensation for the non-orthogonality between x and y axes of the affine transformation.

The general remarks of the DLT can be summarized as follows (Habib, 2000):

- The equations are linear. Thus, we do not need to compute the partial derivatives. Also, approximations for the unknowns are not required.
- It is a special case of RFM of which numerator and denominator are the 1st order and denominators are the identical to each other.
- However, it requires at least 6 control points distributed well in 3D space and the solution is very sensitive to the configuration of the control points in the object space.
- The accuracy of the results is lower than that of collinearity based rigorous model.

3. Experiments and Results

3.1 Simulation of Push-broom Image Acquisition

Based on the rigorous model which considers the dynamic conditions of imaging procedure into the formulation of EOP, the foot print and the image coordinates of push broom scanner are simulated. Table (1) shows the parameters are assumed and set as input

Table 1. Input parameters for simulating push-broom scanner image.

Parameters	Left Image	Right Image
(x_p, y_p) [mm]	(0.0, 0.0)	(0.0, 0.0)
(ω, ϕ, κ) [deg]	(0.0, 0.0, 0.0)	(0.0, 0.0, 0.0)
X^t_o [m]	500 + 10 t	1500 + 10 t
Y^t_o [m]	50 + 10 t	50 + 10 t
Z^t_o [m]	680,000	680,000
Image size	(18,805 × 14,159)	(18,805 × 14,159)

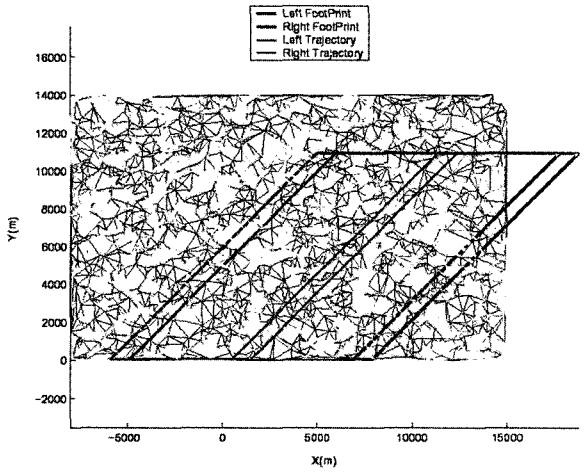

Fig. 3. The foot prints of left and right image of push-broom scanner.

for simulation.

For the simulation, only two EOP parameter, X^t_o and Y^t_o, are assumed as 1st order polynomials with respect to scan time and the rest of EOP are assumed as constant:

$$X^t_o = X_o + \triangle_1 t$$
$$Y^t_o = Y_o + \triangle_2 t \qquad (29)$$

Where, (X^t_o, Y^t_o) are the X-Y ground coordinates of perspective center of scanner at arbitrary time of scan, t = t, (Xo, Yo) are the X-Y ground coordinates of perspective center of scanner at starting time of scan, t = 0, (Δ_1, Δ_2) are the incremental coefficients with respect to scan time.

The simulated foot prints of push-broom scanner are shown in figure (3) acquired from simulated DEM through parameters shown in table (1).

The left and right push-broom image coordinates corresponding to the ground coordinates of captured foot prints could be computed by using the collinearity equations in shown equations (3) and (4). Figure (4) shows the image coordinates of captured ground points.

Total 826 points and 806 points are captured in left image and right image, respectively. For the evaluation of each sensor model we use a half of points as control points (e.g. 413 points for left image and 403 points for right image) and rest of them as check points.

3.2 Single Photo Resection

In this section, we evaluate the capability of each model by checking the RMS error (pixel unit) of control points and check points. This process is the most fundamental process to illustrate how models well describe the relationship between image space and object space. With simulated image and ground coordinates, we add Gaussian noises on both image coordinates and ground coordinates of points captured. The amounts of noises added are 0～1 pixel (0～10 μm) and 0～1 m for image coordinates and ground coordinates, respectively. In order to estimate parameters involved in each model, we applied least square adjustment, which minimizes the square sum of residuals, by using Gauss-Markov model as follows:

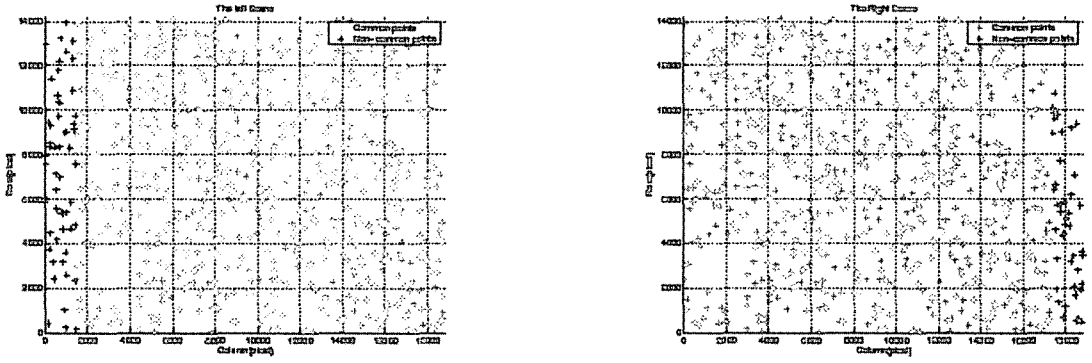

(A) (B)

Fig. 4. Simulated push-broom image coordinates: (A) Left image, (B) Right image.

$$y_{n\times 1} = A_{n\times m} \cdot \xi_{m\times 1} + e_{n\times 1},\ e \sim (0,\ \sigma_o^2 P^{-1}) \quad (30)$$

Where, y_{nx1} is observation vector, A_{nxm} is design matrix consisting of partial derivatives of observations with respect to parameters, ξ_{mx1} is parameter vector to be estimated, e_{nx1} is random error vector, n is number of observation, m is number of parameters to be estimated, P is weight matrix of observation.

For the full rank of matrix A, the least square solutions can be expressed as follows (Schafflin, 1999):

$$\begin{aligned} &\xi = N^{-1} c,\ [N,\ c] = A^T P[A, y] \\ &D\xi = \sigma_o^2 N^{-1} \\ &\hat{\sigma}_o^2 = \tilde{e}^T P \tilde{e}/(n-m) \end{aligned} \quad (31)$$

Once we estimate parameters involved in each model, we can project all simulated ground points onto the image space through model. Table (2) shows the number of parameters involved in each model, the required number of control points to estimate parameters, and the results of single photo resection.

When compared with the Affine transformation and DLT, RFM produces slightly improved accuracy (approximately 0.040.05 pixels) of results of single photo resection. However, one thing should be notified we need to manipulate the normal matrix by adding identity matrix multiplied by regularization coefficient α when we estimate polynomial coefficients of RFM. Since the normal matrix is unstable state resulted from sparsity or over-parameterization, the regularization step is needed to make normal matrix is rather stable. The following equation (32) describes how to manipulate the normal matrix.

$$\begin{aligned} &(N + \alpha \cdot I)\tilde{\xi} = A^T P y \\ &\tilde{\xi} = (N + \alpha \cdot I)^{-1} A^T P y \end{aligned} \quad (32)$$

Where, N is normal matrix, I is identity matrix, and α is regularization coefficiient of which range is 0.0000004~0.0064 (Tao and Hu, 2000b).

In this research, we determined the regularization coefficient *a* through iterative process. The criteria of selecting regularization coefficient is that the variance component is getting smaller and converged. Figure 5 illustrates the change of variance component according

Table 2. Results of single photo resection.

Model	Affine		DLT		RFM	
Image	Left	Right	Left	Right	Left	Right
No. of Parameters	8		11		78	
No. of GCP Required	4		6		39	
$\hat{\sigma}_o$	0.62343	0.64100	0.62559	0.63685	0.58969	0.58091
Control Pts. RMSx [Pixel]	0.72778	0.77028	0.72954	0.76243	0.63144	0.63368
Control Pts. RMSy [Pixel]	0.49004	0.46933	0.48997	0.46776	0.48069	0.45611
Control Pts. RMSR [Pixel]	0.87739	0.90200	0.87881	0.89448	0.79359	0.78076
Check Pts. RMSx [Pixel]	0.79313	0.75347	0.79513	0.75026	0.71679	0.69717
Check Pts. RMSy [Pixel]	0.46142	0.47196	0.46169	0.47178	0.48325	0.47919
Check Pts. RMST [Pixel]	0.91759	0.88908	0.91945	0.88626	0.86448	0.84597

(A) Left image case (B) Right image case

Fig. 5. Variance Components according to iteration.

to iteration (e.g. a is started from 0:0001 and decreased until 0.000005 with Δa = 0.000005).

4. Discussion and Conclusion

In this research, the capability of RFM is compared with Affine transformation and DLT by using simulation data. Experiment results proved the feasibility of RFM which can be used as another approximation of rigorous model of linear scanner sensor. However, there are some limitations of using RFM as generic sensor model:

- Compared to other approximations (e.g. Affine transformation and DLT) of sensor model, RFM is slightly improved the accuracy of single photo resection. But, one might argue that the differences are not significant (0.04 ~ 0.05pixels).
- RFM requires too many control points to estimate parameters for imagery of which polynomial parameters (or RFM coefficients) are not provided (e.g. SPOT). This may cause unfeasibility of using RFM for the area which does not have plenty of control points.
- It is necessary to implement regularization step for normal matrix when RFM is used.
- RFM is approximation of physical sensor model, it does not provide any physical interpretation of sensor. This can hinder tracking error source which can be eliminated by error modelling.
- Since RFM has 78 parameters involved in the ratios of 3rd order polynomials, it is susceptible to be over-parameterization which can cause the high correlation between RFM coefficients and instability of the solution.

Future work should focus on more elaborate testing of RFM comparing other models by using real image data. Also, the method of decorrealting the parameters involved in RFM will be studied. Finally, the optimized form of RFM would be proposed according to the various image data contents.

Reference

1. Di, K., Ma, R. and Li, R. (2000). Deriving 3-D shorelines from high resolution IKONOS satellite images with rational functions, Proceeding of ASPRS Annual Convention, Washington D.C., May 22-26.
2. Dowman, I. and Dollo? J.T. (2000). An evaluation of rational function for photogrammetric restitution, IAPRS, Vol. XXXIII, Part B3, Amsterdam, pp. 254-266.
3. El-Manadili, Y. and Novak, K. (1996). Precision rectification of SPOT imagery using the direct linear transformation model, PE & RS, Vol. 62, No. 1, January, pp. 67-72.
4. Habib, A. (2000). GS 628 Class notes, Dept. of Civil and Environment Engineering and Geodetic Science, The Ohio State University.
5. Lee, Y. (2002). Pose estimation of line cameras using linear features, Ph. D. Dissertation of Dept. of Civil and Environment Engineering and Geodetic Science, The Ohio State University.
6. OGC (1999). The OpenGISTM Abstract Specification. Topic 7: The Earth Imagery Case Ver. 4.0, http://www.opengis.org/public/abstract/99-107.pdf.
7. Okamoto, A., Ono, T., Akamatsu, S., Fraser, C., Hattori and S., Hasegawa, H. (1999). Geometric characteristics of alternative triangulation models for satellite imagery. Proceedings of 1999 ASPRS annual Conference, Oregon, May 17-21.
8. Schafflin, B. (1999). GS 650 Class notes, Dept. of Civil and Environment Engineering and Geodetic Science, The Ohio State University.
9. Tao, V.C., Hu, Y., Mercer, J.B., Schnick, S. and Zhang, Y. (2000a). Image rectification using a generic sensor model-rational function model, IAPRS, Vol. XXXIII, Part B3, Amsterdam, pp. 874-881.
10. Tao, V.C. and Hu, Y. (2000b), Investigation of the rational function model. Proceeding of ASPRS annual Convention, Washington D.C.
11. Yang, X. (2000), Accuracy of rational function in photogrammetry. Proceeding of ASPRS Annual Convention, Washington D.C., May 22-26.